ACUSTICA · acta acustica
Vol. 83 (1997) 1039 – 1044

The Active Control of Wall Impedance

D. Thenail, O. Lacour, M. A. Galland, M. Furstoss
Laboratoire de Mécanique des Fluides et d'Acoustique UMR CNRS 5509, Ecole Centrale de Lyon BP163, 69131 Ecully Cedex, France

Summary
In the context of active noise control via impedance changes, we study the classical problem of a one-dimensional wave guide terminated by one source at each end. One of them produces the unwanted disturbance, while the impedance presented by the other is actively controlled in order to achieve the best noise reductions throughout the tube.

PACS no. 43.50.Ki, 43.20.Mv

1. Introduction

It has long been recognized that active control can prevent acoustic power radiation by an unwanted (primary) noise source as well as promoting the absorption of power by the controlled secondary source. Theoretical observations by Ffowcs Williams about active control energetics clearly showed this possibility [1], and hence, different strategies for active noise control could be considered. The relevance of some of them in silencing one-dimensional fields were studied and experimented by Curtis *et al.* ([2] and [3]) and they founded that the optimal strategy involved the primary source becoming unloaded. This was followed by many investigations on enclosed sound fields e.g. Elliott *et al.* [4], Nelson *et al.* [5] and Johnson and Elliott [6].

In this paper, we make a new contribution to the one-dimensional case that has also been the model for many fundamental studies since Guicking *et al.* [7] first chose it: Orduña-Bustamante and Nelson [8], Nicholson and Darlington [9], and Thenail [10]. Our approach solves some practical problems met in the implementation of control systems, the impossibility of performing the spatial sampling of error sensors in the controlled space, for example: active impedance control may be related to recent works adressing global control via the processing of remote error sensors (Elliott *et al.*, [11]). In what follows, the performance of the active control system is not analysed in terms of the adjustment of the secondary source strength, but in the adjustment of the acoustic impedance of the secondary source. We find that at a resonance frequency, the total time-averaged energy is minimised when *the secondary source presents a null impedance.* We also pay attention to practical constraints which dictate that the controlled impedances of our experiments must be real and positive and can not depend on frequency. Under these conditions, we show via a two frequencies excitation example that the maximum energy absorbing impedance may provide the best global sound attenuation.

Our approach is confined to the time-averaging technique and does not address the initial conditions. All the implications of the transient build-up of waves, which have been investigated by Hirami in the context of wave suppression on a string ([12] and [13]), remain.

Received 3 May 1996,
accepted 31 October 1996.

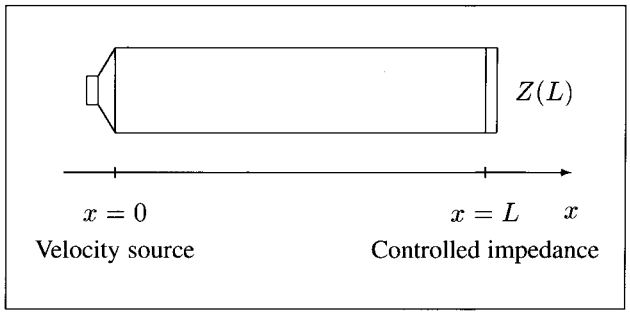

Figure 1. One-dimensional cavity.

2. Analytical description

2.1. Analysis

Only plane waves can propagate in the cavity of length L represented in Figure 1.

A primary source is positioned at the left while a secondary loudspeaker, whose surface acoustic impedance is actively controlled, is at the right. The primary source is a piston which vibrates harmonically with a velocity v_0. The problem of silencing the cavity has been investigated by Curtis *et al.* [2] via the active control of the secondary source strength. An optimal value has been determined and its effects have been compared with those of two other strategies, namely the "acoustical virtual earth" (a terminal pressure release) and the anechoidal termination. The controlled variable in our work is the acoustic impedance of the secondary and we will, via this simple extension, show previous findings in a different light, allowing us to treat very clearly the energetics of the system investigated. We adopt the time dependence $e^{j\omega t}$, and denote k the wave number ω/c_0, c_0 the sound speed, ρ_0 the mass density and $Z_0 = \rho_0 c_0$ the air impedance. The boundary conditions at each end are:

$$\begin{aligned} v(0) &= v_0, \\ p(L)/v(L) &= Z(L). \end{aligned} \tag{1}$$

ACUSTICA · acta acustica
Vol. 83 (1997)

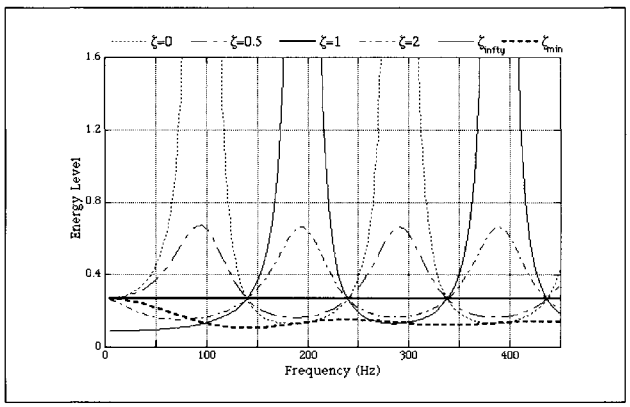

Figure 2. Variation of the time-averaged kinetic energy with the frequency.

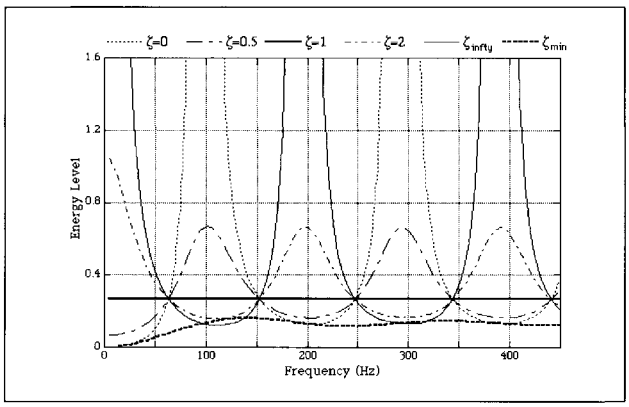

Figure 3. Variation of the time-averaged potential energy with the frequency.

The reduced impedance being defined by $\zeta(x) = Z(x)/Z_0$, the acoustic pressure and velocity are:

$$\begin{aligned} p(x) &= Z_0 v_0 \Big[\big(1+\zeta(L)\big)\, \mathrm{e}^{\mathrm{j}k(L-x)} \\ &\quad - \big(1-\zeta(L)\big)\, \mathrm{e}^{-\mathrm{j}k(L-x)} \Big] \\ &\quad \times \Big[\big(1+\zeta(L)\big)\, \mathrm{e}^{\mathrm{j}kL} \\ &\quad + \big(1-\zeta(L)\big)\, \mathrm{e}^{-\mathrm{j}kL} \Big]^{-1}, \end{aligned} \tag{2}$$

$$\begin{aligned} v(x) &= v_0 \Big[\big(1+\zeta(L)\big)\, \mathrm{e}^{\mathrm{j}k(L-x)} \\ &\quad + \big(1-\zeta(L)\big)\, \mathrm{e}^{-\mathrm{j}k(L-x)} \Big] \\ &\quad \times \Big[\big(1+\zeta(L)\big)\, \mathrm{e}^{\mathrm{j}kL} \\ &\quad + \big(1-\zeta(L)\big)\, \mathrm{e}^{-\mathrm{j}kL} \Big]^{-1}. \end{aligned} \tag{3}$$

Then, it is straightforward to derive the time-averaged kinetic, potential and total energies in the wave guide:

$$\begin{aligned} \overline{E_k} &= \frac{\rho_0 v_0^2}{4} \Big[\big(1+|\zeta(L)|^2\big)L + \big(1-|\zeta(L)|^2\big)\frac{\sin 2kL}{2k} \\ &\quad + \mathrm{j}\big(\zeta(L)-\zeta^*(L)\big)\frac{1-\cos 2kL}{2k} \Big] \\ &\quad \times \Big[1+|\zeta(L)|^2 + \big(1-|\zeta(L)|^2\big)\cos 2kL \\ &\quad + \mathrm{j}\big(\zeta(L)-\zeta^*(L)\big)\sin 2kL \Big]^{-1}, \end{aligned} \tag{4}$$

$$\begin{aligned} \overline{E_p} &= \frac{\rho_0 v_0^2}{4} \Big[\big(1+|\zeta(L)|^2\big)L \\ &\quad - \big(1-|\zeta(L)|^2\big)\frac{\sin 2kL}{2k} \\ &\quad - \mathrm{j}\big(\zeta(L)-\zeta^*(L)\big)\frac{1-\cos 2kL}{2k} \Big] \\ &\quad \times \Big[1+|\zeta(L)|^2 + \big(1-|\zeta(L)|^2\big)\cos 2kL \\ &\quad + \mathrm{j}\big(\zeta(L)-\zeta^*(L)\big)\sin 2kL \Big]^{-1}, \end{aligned} \tag{5}$$

$$\begin{aligned} \overline{E_{tot}} &= \frac{\rho_0 v_0^2 L}{2} \Big[\big(1+|\zeta(L)|^2\big) \Big] \\ &\quad \times \Big[1+|\zeta(L)|^2 + \big(1-|\zeta(L)|^2\big)\cos 2kL \\ &\quad + \mathrm{j}\big(\zeta(L)-\zeta^*(L)\big)\sin 2kL \Big]^{-1}. \end{aligned} \tag{6}$$

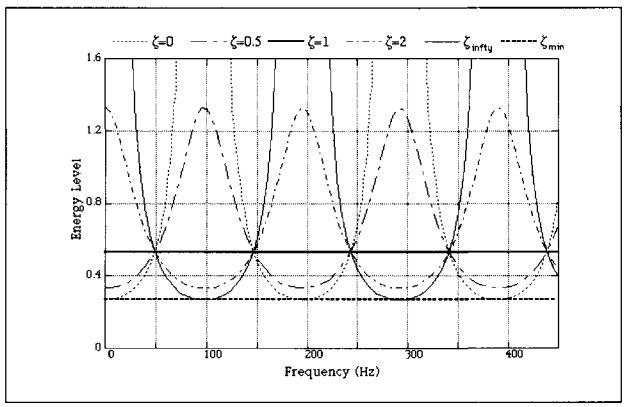

Figure 4. Variation of the time-averaged total energy with the frequency.

Both time-averaged kinetic and potential energies tend to be equal to one half of the total energy as frequency increases. Figures 2, 3 and 4 give their respective evolutions with the frequency, for different terminal impedances. It comes out that as soon as frequency exceeds the first anti-resonance, the kinetic, potential and total energies have the same shape, for any terminal impedance value. The potential energy provides a suitable information about the evolution of the total energy we will exploit in our experiments, like in the referenced prior works.

2.2. The optimal impedance

The determination of the extrema of the time averaged total energy (expression 6) as a function of the terminal impedance is straightforward. The maxima are given by:

$$\zeta_{LMax} = \mathrm{j}\cot an\, kL, \tag{7}$$

while the minima are:

$$\zeta_{Lmin} = -\mathrm{j}\,\tan\, kL. \tag{8}$$

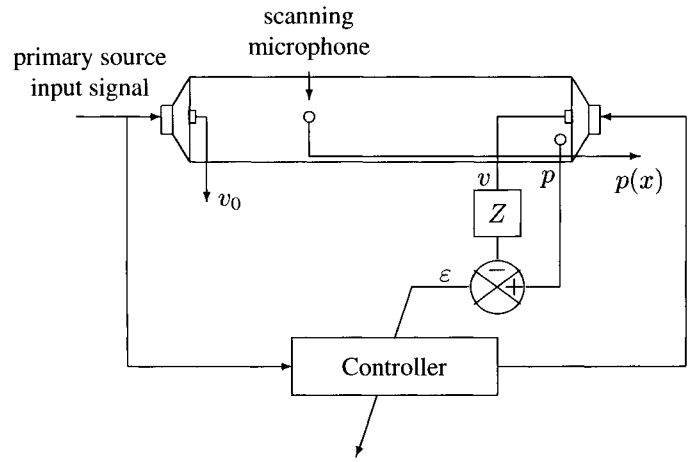

Figure 5. Experimental set-up.

The latter expression (also obtained by Darlington and Avis [14]) may be deduced from the optimal strategy defined by Curtis *et al.*, namely $v(L) = v(0)\cos kL$, recognizing that:

$$Z(L) = H^{-1}Z_{ps} + Z_{ss}, \tag{9}$$

where Z_{ss} is the secondary source radiation impedance, Z_{ps} is the primary to secondary transfer impedance, $H = -v(L)/v(0)$ is the sources strength ratio.

The energetics of the system terminated by the optimal impedance is examined via the impedance transfer formula:

$$\zeta(0) = \frac{-\mathrm{j}\zeta(L)\operatorname{cotan} kL + 1}{\zeta(L) - \mathrm{j}\operatorname{cotan} kL}. \tag{10}$$

Thus, the terminal impedance $\zeta_{Lmin} = -\mathrm{j}\tan kL$ at $x = L$, which leads to energy minima, is the impedance which gives $\zeta(x) = 0$ at $x = 0$ and the time-averaged acoustic intensity at the primary source is exactly zero. We have refound in a simple way that the "optimal" impedance neither supplies nor absorbs any power, while also preventing sound power radiation by the primary source. The maximally absorbent impedance $\zeta(L) = 1$ presents the interesting feature of flattening the guide's acoustic response, thus reducing the potentially damaging effect of resonances, but does not allow the energy in the tube to be minimum.

As seen above, the optimal impedance ζ_{Lmin} is frequency dependent and the particular cases of the rigid cavity resonances and anti-resonances will now be considered. At a tube's resonance ($kL = n\pi$), the expression (8) reduces to $\zeta_{Lmin} = 0$, and the impedance approach shows clearly that a pressure release at $x = L$ allows the best global sound attenuation in the tube. At anti-resonances ($kL = (2n+1)\pi/2$), the terminating infinite impedance is the optimal boundary condition, while a null impedance causes the total time-averaged energy to be infinite. If we consider the control of any other frequency, the experimental achievement of the imaginary and frequency dependent optimal impedance ζ_{Lmin} is more difficult. It is seen from Figure 4 that $\zeta(L) = 1$ provides good energy reduction in the frequency region close to a resonance but creates some amplification when the excitation frequency is close to an anti-resonance. These relatively mediocre performances become the best which can be obtained when one resonance and one anti-resonance are simultaneously and equally excited, as will be experimented below. In addition, it is likely that this strategy, even somewhat suboptimal, is the attractive compromise to be applied in real situations including significantly broadband excitations.

3. Experiments

In order to illustrate some of the results presented above, we exploit a set-up previously designed for active impedance control experiments in an impedance tube [15], [9].

3.1. Set-up

The cavity is a 0.88m long square hard-walled tube, terminated at each end by two identical loudspeakers. They represent the velocity source, and the controlled impedance, respectively. Their square flat membrane fills almost exactly the tube cross section (0.12m×0.12m). For the experimental frequencies, the tube is one-dimensional, even very closely to each loudspeaker. In the preceding section, the velocity of the primary source is assumed to be constant. Thus, an accelerometer of negligible mass is put on its membrane in order to balance the loudspeaker efficiency which varies with the frequency and the acoustic load presented by the cavity (preliminary experiments have taught us that this point was of great importance). The acoustic impedance at the membrane of the secondary loudspeaker is controlled via another accelerometer and a microphone. The "Filtered-X" LMS algorithm is implemented on a numerical filter whose input is the electric signal which feeds the primary source. The secondary signal which is delivered at the output is amplified and connected to the secondary source. The energy of the error signal $\varepsilon = p - Zv$ is minimized, and the impedance Z is produced. The acoustic field inside the tube along its axis is scanned via a microphone, which allows also a supplementary check of the terminal impedance value via a variation

ACUSTICA · acta acustica
Vol. 83 (1997)

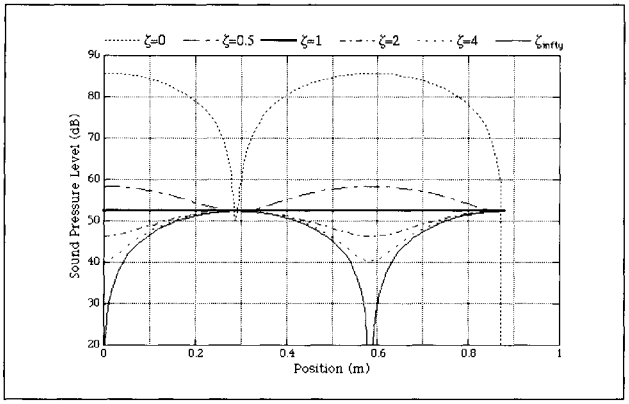

Figure 6. Sound pressure level variation along the tube axis near an anti-resonance at $f = 291$ Hz. Calculations.

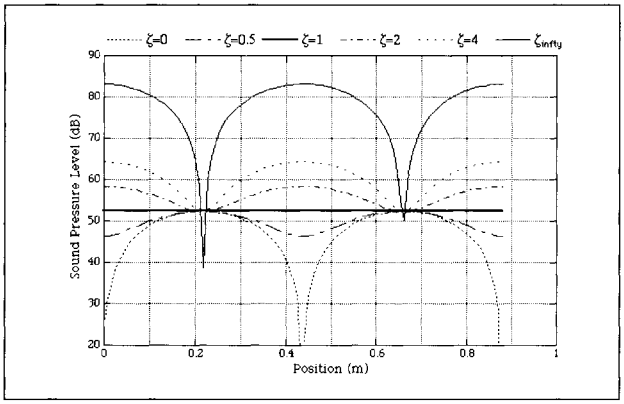

Figure 8. Sound pressure level variation along the tube axis near a resonance at $f = 388$ Hz. Calculations.

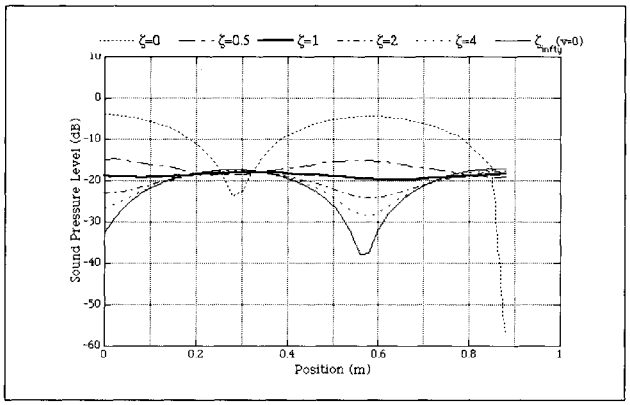

Figure 7. Sound pressure level variation along the tube axis near an anti-resonance at $f = 291$ Hz. Measurements.

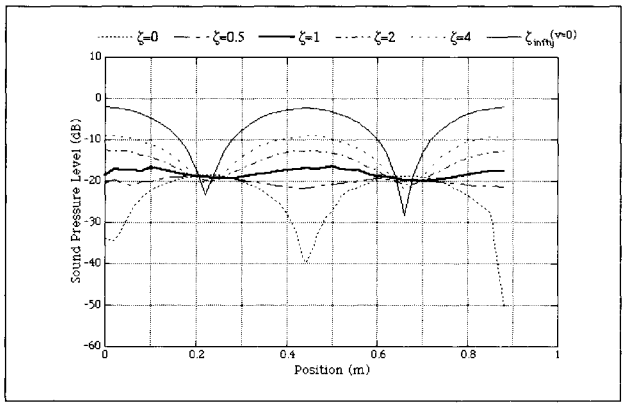

Figure 9. Sound pressure level variation along the tube axis near a resonance at $f = 388$ Hz. Measurements.

of Chung and Blaser's method [16], presented by Chu [17]. Finally, it has been seen in the preceding section that for frequencies exceeding the first anti-resonance of 97 Hz, the time-averaged total and potential energies tend to be proportional. Consequently, the evolution of potential energy may be used to describe the total energy variations. Like in Curtis *et al.*, we use the indicator of the sum of the mean squared sound pressures sensed along the tube axis,

$$J_p = \sum_{i=1}^{N} p_i^2. \tag{11}$$

Figure 5 represents the overall experimental set-up.

3.2. Control near an anti-resonance at $f = 291$ Hz

Figure 6 represents the sound pressure level inside the tube according to expression (2), for different terminal impedances, while the corresponding experimental measurements are shown in Figure 7. A good agreement is generally observed and confirms that a strictly local pressure release may involve large pressure levels everywhere else in the tube. The discrete sum of mean squared levels and the impedance measured via the Chu's method are reported in Table I.

It comes out from the figures that actual sound levels should be much higher for $\zeta(L) = 0$. The impedance achieved at the guide termination is not exactly zero and introduces a weak damping which is sufficient to explain the main discrepancy between measurements and results from expression (2).

3.3. Control near a resonance at $f = 388$ Hz

The expected sound pressure levels are reported in Figure 8, while the measurements and the estimated potential energy in the guide are shown in Figure 9, and in Table II, respectively. In this case, the null impedance is the impedance which allows the best global sound reduction in the tube. This result is clear: assigning an active pressure release at the end of our guide is equivalent to adding a "virtual" $\lambda/4$ length, in such a way that an initially resonant frequency presents now an anti-resonant behaviour.

3.4. Control of both frequencies

We report here the control of a particular signal composed of one resonance and one anti-resonance equally excited. The calculated sound pressure levels are shown in Figure 10,

Table I. Estimation of the potential energy in the guide excited near an anti-resonance at $f = 291$ Hz, for different terminal impedances.

ζ_{Th}	0	0.5	1	2	4	∞
ζ_{Mes}	$< 0.1 + j0.1$	$0.6 - j0.0$	$1.2 + j0.1$	$2.1 + j0.6$	$3.7 + j0.8$	$5.6 + j7.4$
J_p	9.3 dB	−0.2 dB	−2.4 dB	−3.4 dB	−3.7 dB	−3.8 dB

Table II. Estimation of the potential energy in the guide excited near a resonance at $f = 388$ Hz, for different terminal impedances.

ζ_{Th}	0	0.5	1	2	4	∞
ζ_{Mes}	$< 0.1 + j0.1$	$0.6 - j0.1$	$1.3 - j0.1$	$2.3 + j0.2$	$4.6 + j0.6$	$0.2 + j13.4$
J_p	−5.1 dB	−3.6 dB	−1.6 dB	1.5 dB	4.7 dB	11.3 dB

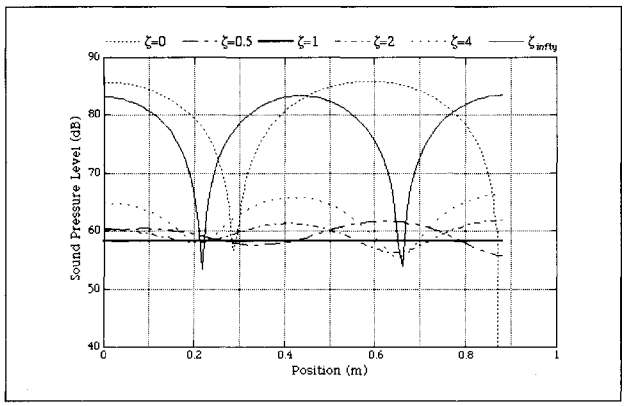

Figure 10. Sound pressure level variation along the tube axis. Two frequencies excitations: $f_1 = 291$ Hz, $f_2 = 388$ Hz. Calculations.

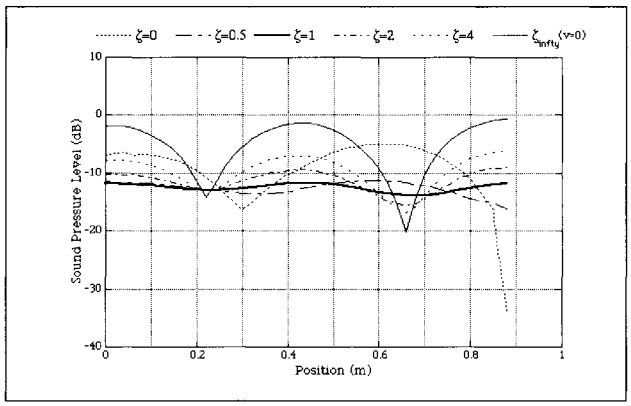

Figure 11. Sound pressure level variation along the tube axis. Two frequencies excitations: $f_1 = 291$ Hz, $f_2 = 388$ Hz. Measurements.

Table III. Estimation of the potential energy in the guide, when simultaneously and equally excited at $f = 291$ Hz and at $f = 388$ Hz.

Impedance ζ	0	0.5	1	2	4	∞
J_p [dB]	8.6	4.0	3.9	5.3	7.3	12.47

while the measurements and the estimated potential energy in the guide are reported in Figure 11 and in Table III, respectively. In the case of positive real impedances, $\zeta(L) = 1$ produces the best global sound attenuation.

3.5. Discussion about the impedances achieved

We point out first that the theoretical case of an infinite impedance has been replaced during the experiments by a zero velocity condition at the controlled loudspeaker.

What mostly explains the differences between the theoretical and measured impedances (Tables I, II, and III) is that acoustic pressure and velocity are not equally delayed by their respective measurement devices before being converted in digital signals updating the controller's coefficients.

The problem of transduction errors in the case of the active anechoic termination has been investigated by Darlington *et al.* [18], and it may be added to the experimental difficulties reviewed in the latter reference (transduction and digital signal processing errors), that the impedance measurement accuracy is also strongly dependent on the desired terminal impedance. In particular, very high and low impedances for which the acoustic field in the guide is very reactive, are more subjected to measurement errors than an absorbing termination.

Finally, the achievement of a given real impedance over wide frequency ranges has also been attempted. The attenuation at each frequency was not significantly different from the attenuation achieved using a single frequency primary signal. However, it clearly confirms from a practical point of view the usefullness of using, as active impedance, a porous layer backed by an active acoustical short-circuit, as experimented first by Guicking and Lorentz [19], then by Thenail *et al.* [20].

ACUSTICA · acta acustica
Vol. 83 (1997)

4. Conclusion

We have demonstrated, via the acoustics of a one-dimensional wave guide, the potentialities of active impedance control in silencing a system. On the one hand, this approach gives clear teachings and completes previous contributions by other authors about the energetics of active control. On the other hand, the given example demonstrates that impedance control gives the same optimal performance as classical feedforward schemes.

In our wave guide, the optimal terminal impedance which minimizes the total energy by preventing power radiation by the primary source, has been experienced near a resonance where the optimal impedance becomes an active pressure release. This work must now account for significantly broadband and unexpected disturbances and will probably show an increasing importance to the design of active absorbers.

Acknowledgement

The authors express their gratitude to Professor J. E. Ffowcs Williams (University of Cambridge, U. K.) for many comments and discussions. D. Thenail is currently post-doctoral fellow of the Centre National d'Etudes Spatiales.

References

[1] J. E. Ffowcs Williams: Anti-sound. Proc. R. Soc. London **395** (1984) 63–88. Ser. A.

[2] A. R. D. Curtis, P. A. Nelson, S. J. Elliott, A. J. Bullmore: Active suppression of acoustic resonance. J. Acous. Soc. Am. **81** (1987) 624–631.

[3] A. R. D. Curtis, P. A. Nelson, S. J. Elliott: Active reduction of a one-dimensional enclosed sound field : An experimental investigation of three control strategies. J. Acous. Soc. Am. **88** (1990) 2265–2268.

[4] S. J. Elliott, P. Joseph, P. A. Nelson, M. E. Johnson: Power output minimization and power absorption in the active control of sound. J. Acous. Soc. Am. **90** (1991) 2501–2511.

[5] P. A. Nelson, J. K. Hammond, P. Joseph, S. J. Elliott: Active control of stationary random sound fields. J. Acous. Soc. Am. **87** (1990) 963–975.

[6] M. E. Johnson, S. J. Elliott: Measurement of acoustic power output in the active control of sound. J. Acous. Soc. Am. **93** (1993) 1453–1459.

[7] D. Guicking, K. Karcher, M. A. Rollwage: Coherent active methods for applications in room acoustics. J. Acous. Soc. Am. **78** (1985) 1426–1434.

[8] F. Orduña Bustamante, P. A. Nelson: An adaptive controller for the active absorption of sound. J. Acous. Soc. Am. **91** (1992) 2740–2747.

[9] G. C. Nicholson, P. Darlington: Active control of acoustic absorption, reflection and transmission. Proc. I.O.A., 1993. 403–409.

[10] D. Thenail: Contrôle actif d'impédance et optimisation des performances d'un matériau poreux. Dissertation. Ecole Centrale de Lyon, 1995. 95-11.

[11] S. J. Elliott, T. J. Sutton, B. Rafaely, M. Johnson: Design of feedback controllers using a feedforward approach. Proc. Active 95, Newport Beach, CA, USA, 1995. 863–874.

[12] N. Hirami: Is the optimal damper a good attenuator ? Proc. Idee-Force EUR'ACOUSTICS, Ecole Centrale de Lyon, 1992. W14.

[13] N. Hirami: Optimal energy absorption for wave suppression. 13ème colloque d'Aéro et Hydroacoustique, Ecole Centrale de Lyon, 1993. 41–45.

[14] P. Darlington, M. R. Avis: Modifying low frequency room acoustics 2 : global control using active absorbers. Proc. I.O.A., 1995. 87–96.

[15] D. Thenail, M. A. Galland: Development of an active anechoidal boundary. Proc. Idee-Force EUR'ACOUSTICS, Ecole Centrale de Lyon, 1992. W4.

[16] J. Y. Chung, D. A. Blaser: Transfer function method of measuring in-duct acoustic properties. J. Acous. Soc. Am. **68** (1980) 907–922.

[17] W. T. Chu: Transfer function technique for impedance and absorption measurements in an impedance tube using a single microphone. J. Acous. Soc. Am. **80** (1986) 555–560.

[18] P. Darlington, G. C. Nicholson, S. E. Mercy: Input transduction errors in active acoustic absorbers. Acta Acustica **3** (1995) 345–349.

[19] D. Guicking, E. Lorentz: An active sound absorber with porous plate. ASME J. Vib. Acoustics, Stress Reliab. Des. **106** (1984) 389–404.

[20] D. Thenail, M. A. Galland, M. Furstoss, M. Sunyach: Absorption by an actively enhanced material. Proc. of the 1994 ASME Winter Annual Meeting, Chicago, Il, USA, 1994. 441–448. AM-16D.